JOURNAL OF APPLIED POLYMER SCIENCE VOL. 12, PP. 939-953 (1968)

Flow Properties of Polyethylene Melt

TADAO KATAOKA and SHIGEYUKI UEDA,
Textile Research Institute of the Japanese Government, Kanagawaku, Yokohama, Japan

Synopsis

Flow properties for low-density and high-density polyethylene over a broad range of shear stress are described. Flow equations presented in literatures are tested from the point of view of the extrapolating method for evaluating the zero shear viscosity. It is shown that the method based on the equation of Cross gives relatively good results. The recoverable shear strain calculated from the capillary end correction is practically equal to that determined from the creep experiment at the same shear stress. The effect of shear stress on the elastic property is examined.

INTRODUCTION

In polymer melt rheology two types of apparatus, a rotational viscometer and a capillary extrusion rheometer, are most frequently used.[1,2] With a rotational viscometer one can determine flow properties under lower shear stress (or shear rate); with a capillary extrusion rheometer, those under higher shear stress (or shear rate). Most of the experimental work presented in the literature were carried out with one type of apparatus, either a rotational[3-5] or a capillary extrusion[6-10] viscometer.

To obtain valid data over a broad range of shear stress (or shear rate) it is effective to determine the flow properties with both apparatuses. In carrying out the experiment it is desirable that the ranges of shear stress (or shear rate) covered with each apparatus overlap each other. Further, if both the elastic properties and the viscous properties are determined with a rotational viscometer, the result may be compared with information on the elastic properties obtained from the capillary rheometer.[2,6] This is the subject of the present investigation.

In this paper experimental work on the flow properties of high- and low-density polyethylene melts is described. A cone–plate viscometer and two capillary extrusion rheometers were used. With the former apparatus viscosity and steady-state compliance were determined as functions of shear stress. With the latter apparatus the total end corrections[2,6] and flow relations[2] were determined.

EXPERIMENTAL

Materials

Seven resins were studied; their characteristics are listed in Table I. Sample Y was an experimentally prepared low-density polyethylene, which was supplied from Mitsubishi Yuka Co. Ltd., and it was shown[11] by column fractionation that its molecular weight distribution curve had a peak on the higher molecular weight side. Other samples were commercial products; the D series samples were low-density (Bakelite type) and the S series samples were high-density (Phillips type) polyethylene. The weight-average molecular weights in column 7 were those calculated from melt viscosity data by using the relations reported by Tung.[5] All samples contained antioxidant of about 0.1%, and appreciable chemical change did not occur during an experimental run.

TABLE I
Description of Samples

Code	Type	Manufacturer	Dens., at 25°C., g./cm.^{3}	$[\eta]^a$	Melt index	$\bar{M}_w{}^b$ ($\times 10^{-4}$)
D-1	DFD-6005	Nitto Yunika Co. Ltd.	0.92	—	0.30	22
D-2	DYNH-3	"	0.92	—	1.75	10.5
D-3	DND-0400	"	0.92	—	20.7	4.0
Y	Yukalon	Mitsubishi Yuka Co. Ltd.	0.92	0.98	2.77	9.5
S-1	Sholex 6002	Showa Yuka Co. Ltd.	0.96	2.10	0.29	20
S-2	Sholex 6015	"	0.96	1.68	1.56	10
S-3	Sholex 6050	"	0.96	1.51	5.05	7.5

[a] Decalin solution at 130°C.

[b] Values of $\bar{M}_w$ were calculated from melt viscosity η by means of following relations:[5] $\log \eta = 3.4 \log \bar{M}_w + (1.64 + 10^3/T) - 15.5$ for high-density samples and $\log \eta = 3.4 \log \bar{M}_w + (3.16 \times 10^3/T) - 19.0$ for low-density samples.

Apparatus

To determine flow properties under lower shear stress a cone–plate viscometer, operated at constant shear stress, was used. The shear stress τ and the shear rate $\dot{\gamma}$ were calculated from the torque M applied and the angular velocity Ω of rotation of the plate by using eqs. (1) and (2):

$$\tau = 3M/2\pi R^3 \tag{1}$$

$$\dot{\gamma} = \Omega/\theta \tag{2}$$

where R is the radius of the cone, and θ is the angle between the cone and the plate. With the same apparatus the creep experiment was carried out,[12] and the steady-state compliance J_e was determined as the ratio of the total recoverable deformation to shear stress.

To obtain flow properties under higher shear stress two piston-driven capillary extrusion rheometers were used; one was a standard Melt Indexer, and the other was a Koka Flow Tester.[13] In the Melt Indexer various loads up to 21.6 kg. were applied, and the value of specific volume necessary to convert the weight of the extrudate to volume was taken from the data of Tung.[14] In the Koka Flow Tester, the construction and use of which is described by Arai,[13] various pressures up to 300 kg./cm.^{2} were applied. The orifices used were made of stainless steel and had flat entries; their dimensions are listed in Table II.

TABLE II
Dimensions of Orifices

	Capillary		
Orifices for:	Length l, mm.	Radius, r, mm.	l/r
Melt indexer	18.83	1.047	18.0
	12.55	1.047	12.0
	8.02	1.047	7.66
Koka flow tester	3.0	0.25	12.0
	2.5	0.25	10.0
	2.0	0.25	8.0
	1.00	0.25	4.0
	1.00	0.50	2.0

Maximum shear stress τ' and shear rate D at the capillary wall were calculated from eqs. (3) and (4):

$$\tau' = rP/2l \tag{3}$$

$$D = 4Q/\pi r^3 \tag{4}$$

where r and l are the radius and length of the orifice, respectively, Q is the volumetric flow rate, and P is the applied pressure.

For viscoelastic and non-Newtonian liquid true values of shear stress τ and shear rate $\dot{\gamma}$ are calculated from eqs. (5) and (6):

$$\tau = rP/2(1 + er) \tag{5}$$

$$\dot{\gamma} = D(3/4 + b/4) \tag{6}$$

where e is the total end correction[6] and b is $(d \log D)/(d \log \tau')$.

Experiments for sample D-2 were carried at 130, 152, 190, 220°C., and those for other samples were carried at 152°C. only. In this paper the results with no particular indication of temperature are those obtained at 152°C.

RESULTS

Samples D-1 and S-1 were taken to show typical results. The results with the cone–plate viscometer are given in Table III, where shear rate $\dot{\gamma}$,

viscosity η ($\equiv \tau/\dot{\gamma}$), and steady-state compliance J_e at various shear stresses τ are listed. It was rather difficult to determine J_e with accuracy. The values given in the table are the arithmetic averages of three measurements. In Table IV all data obtained with capillary rheometers are given at various levels of D. For sample S-1 values of $\dot{\gamma}$ and η in the range of $10^2 < D < 10^3$ sec.$^{-1}$ were not determined, because of the discontinuity in the flow curve.

Characteristic features of flow curves are shown in Figure 1. The arrow in this figure represents the point of the critical shear stress τ_d, above which

TABLE III
Viscosity and Steady-State Compliance for Sample D-1 and S-1 at 152°C.

τ, dynes/cm.^{2} ($\times 10^{-3}$)	Sample D-1			Sample S-1		
	$\dot{\gamma}$, sec.$^{-1}$ ($\times 10^3$)	η, poise ($\times 10^{-6}$)	J_e, cm.^{2}/dyne ($\times 10^6$)	$\dot{\gamma}$, sec.$^{-1}$ ($\times 10^3$)	η, poise ($\times 10^{-6}$)	J_e, cm.^{2}/dyne ($\times 10^6$)
0.707	0.186	3.80	6.5	0.364	1.94	2.0
1.07	0.315	3.40	6.8	0.548	1.95	1.8
1.84	0.552	3.33	6.8	0.943	1.95	2.0
3.80	1.15	3.32	5.9	1.94	1.96	1.8
7.55	2.45	3.08	6.0	4.44	1.70	1.8
11.6	5.00	2.32	4.6	7.48	1.55	2.0
20.7	9.02	2.30	3.2	17.6	1.18	2.2
33.0	16.0	2.06	3.1	31.1	1.06	2.0
45.0	31.0	1.45	3.0	52.3	0.86	1.7
61.7	47.2	1.30	2.6	100	0.617	1.7

the appearance of the extrudate became irregular. The flow irregularity was not observed for sample D-3. Flow curves for low-density samples are continuous over the shear stress range studied. For high-density samples discontinuities in the flow curves are shown. The flow irregularity for high-density samples seems to start at the shear stress at which the discontinuity occurs. Flow properties above τ_d for samples S-2 and S-3 were not determined. Values of τ_d are given in column 3 of Table V.

Flow properties of sample D-2 were determined at four temperatures. The data were reduced to temperature, as shown in Figure 2. The superposition of data points is satisfactory even in the region of irregular flow.

The variation of total end correction e with shear rate D (uncorrected value) is shown in Figure 3. The arrow in this figure represents the point of the onset of the irregular flow. These curves are similar to those reported in the literature. The values of e for low-density samples are much larger than those of high-density samples and seem to converge to a limiting value. The increase in temperature shifts the curve to a higher shear rate.

TABLE IV
Results of Capillary Rheometry for Samples D-1 and S-1 at 152°C.[a]

	Sample D-1					Sample S-1				
D	b	$\dot{\gamma}$	τ	η	e	b	$\dot{\gamma}$	τ	η	e
0.01	1.20	0.0105	0.191	18.2	1.5	1.24	0.0106	0.133	12.5	1.0
0.02	1.35	0.0218	0.330	15.1	1.7	1.33	0.0216	0.226	10.5	1.0
0.04	1.58	0.0458	0.538	11.7	2.0	1.40	0.0440	0.37	8.41	1.1
0.1	1.94	0.1235	0.91	7.37	2.5	1.63	0.116	0.67	5.77	1.3
0.2	2.06	0.253	1.33	5.26	3.7	1.70	0.234	1.02	4.35	1.45
0.4	2.12	0.512	1.84	3.59	4.6	1.78	0.496	1.53	3.21	1.7
1.0	2.31	1.33	2.72	2.05	6.4	1.83	1.21	2.58	2.13	2.0
2.0	2.50	2.75	3.7	1.35	7.5	2.02	2.52	3.6	1.43	2.3
4.0	2.71	5.71	4.8	0.841	8.3	2.26	5.28	5.0	0.947	2.5
10	3.13	15.3	6.5	0.424	9.1	2.56	15.9	7.2	0.518	2.95
20	3.13	30.6	8.1	0.265	9.6	2.56	27.8	9.5	0.342	3.3
40	3.13	61.2	10.2	0.168	9.8	2.56	55.6	12.3	0.221	3.7
100	3.13	153	17.3	0.091	10.1	2.56	139	15.3	0.157	4.1
200	3.13	306	21.7	0.057	10.3	—	—	—	—	(5.1)
400	3.13	612	26.0	0.035	10.5	—	—	—	—	(6.2)
1,000	3.13	1,530	29.1	0.019	10.8	1.56	1140	22.5	0.02	9.2

[a] D, sec.$^{-1}$; $b \equiv (d \log D)/(d \log \tau')$; τ, dynes/cm.^{2} ($\times 10^{-5}$); η, poise ($\times 10^5$).

TABLE V

Critical Shear Stress τ_d, Zero Shear Viscosity η_0, Steady-State Compliance J_e, Shear Modulus μ, and Internal Shear Modulus of Rigidity, G_i

Sample no.	Temp., °C.	τ_d, dynes/cm.^{2} ($\times 10^{-5}$)	η_0, poises ($\times 10^{-5}$)		J_e, cm.^{2}/dyne ($\times 10^5$)	μ, dynes/cm.^{2} ($\times 10^{-4}$) at τ, in dynes/cm.^{2}, equal to:		G_i, dynes/cm.^{2} ($\times 10^{-4}$)
			Obsd.	Calcd.		10^5	10^6	
D-1	152	6	36	33	6.4	2.0	5.5	3.6
D-2	130	7	8.4	7.8	3.0	3.0	7.0	5.9
"	152	7	3.4	2.8	3.0	3.3	7.3	5.0
"	190	7	1.2	0.9	—	3.2	7.0	6.0
"	220	8	0.46	0.33	—	3.5	6.8	6.2
D-3	152	—	0.145	0.132	—	5.1	10.5	14.5
Y	152	9	2.6	1.13	1.5	3.7	5.9	4.0
S-1	152	20	19.5	11	2.0	7.5	19	2.8
S-2	152	(25)	3.1	1.21	2.0	8.5	27	3.1
S-3	152	(25)	0.95	0.40	1.6	8.0	31	4.1

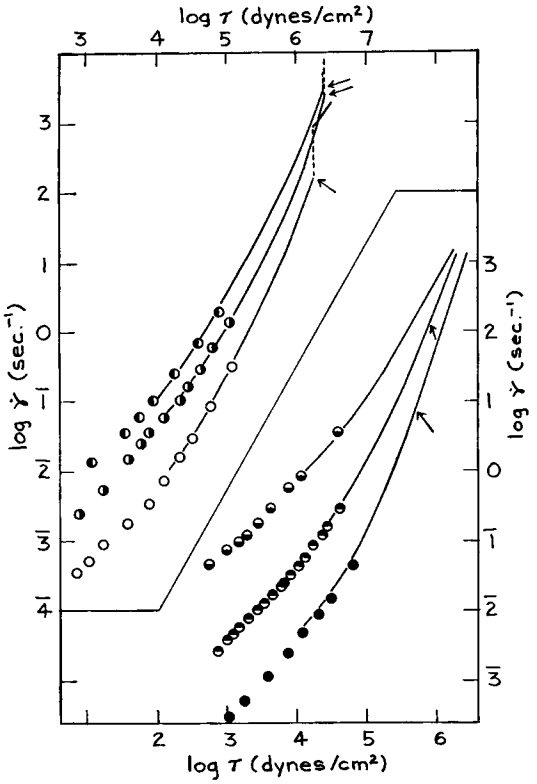

Fig. 1. Shear rate versus shear stress at 152°C. for sample: (O) S-1; (◑) S-2; (◐) S-3; (●) D-1; (◒) D-3; (◓) Y. Data points are those obtained with the cone–plate viscometer; and curves are from the capillary rheometry. The arrow represents the point of the onset of irregular flow.

DISCUSSIONS

Extrapolating Method of Estimating Zero Shear Viscosity

Many flow equations, theoretical and empirical, have been proposed[15–21] for non-Newtonian liquid. On the basis of those equations one can evaluate the zero shear viscosity η_0 by extrapolating the data at any shear stress (or shear rate.) We examined the applicability of those equations as a method of estimating η_0. From the practical point of view of easy applicability the following methods were tested.

Method 1: plots of $1/\eta$ against τ.
Method 2: plots of log $(1/\eta)$ against τ.
Method 3: plots of $1/\eta$ against $\dot{\gamma}^{2/3}$.

Method 1 is based on Ferry's equation,[22]

$$\eta_0/\eta = 1 + \tau/G_i \tag{7}$$

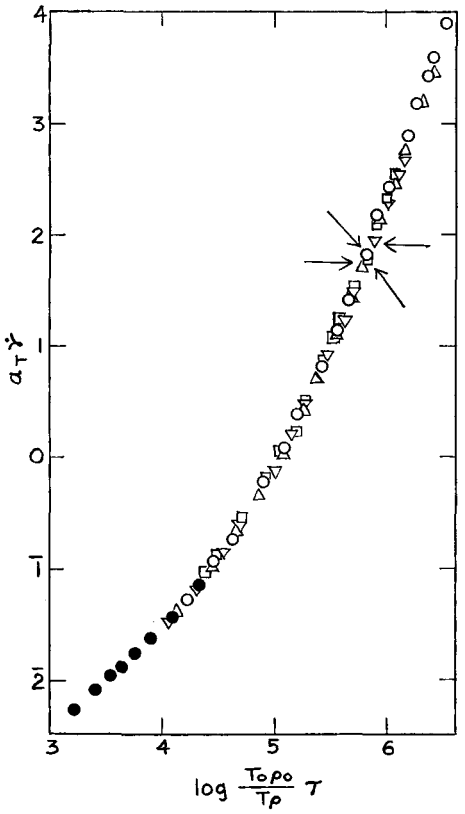

Fig. 2. A composite relationship of shear rate versus shear stress reduced to 152°C. for sample D-2. Capillary data at (temp., °C.): (○) 130; (△) 152; (▽) 190; and (□) 220. Cone–plate data (●) at 130°C.

where G_i is the "internal shear modulus of rigidity." Method 2 is based on the equation

$$\eta_0/\eta = Ae^{B\tau} \tag{8}$$

which was given by Spencer and Dillon[16] as early as 1948. Methods 1 and 2 are frequently used for estimating η_0. Method 3 is based on the equation derived by Cross,[21]

$$\eta = \eta_\infty + \frac{\eta_0 - \eta_\infty}{1 + \alpha\dot{\gamma}^{2/3}} \tag{9}$$

where η_∞ is the viscosity at infinite shear.

Figures 4–6 show plots for samples D-1 and S-1 after the above-mentioned methods. In polymer melt rheology flow data are frequently determined over shear stress from 10^5 to 10^6 dynes/cm.^{2}. Thus, plots in those figures are made to show data at shear stresses below 10^6 dynes/cm.^{2};

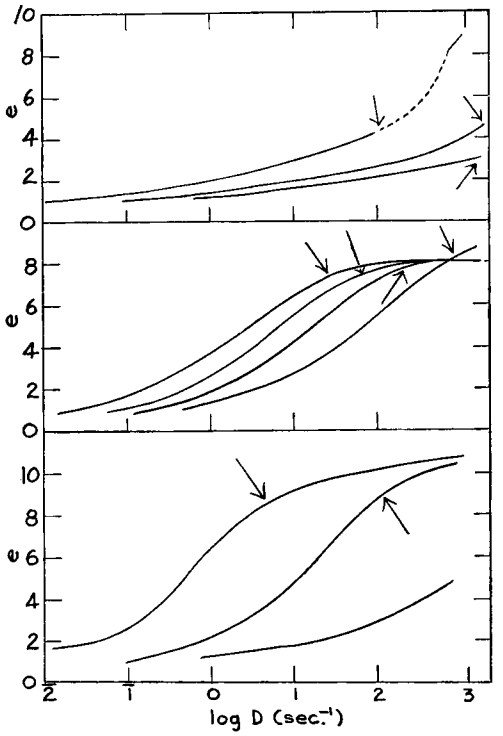

Fig. 3. Total end correction e versus (uncorrected) shear rate D: (*top*) S-1, S-2, and S-3, from left to right; (*middle*) D-2 at 130, 152, 190, and 220°C., from left to right; (*bottom*) D-1, Y, and D-3, from left to right.

data points at lower shear stress (or shear rate) are given in enlarged scale, to show whether the extrapolation is successful.

Plots of method 1 give approximately a straight line at shear stress below about 10^5 dynes/cm.^{2} (Fig. 4*a* for sample D-1) or 3×10^5 dynes/cm.^{2} (Fig. 4*b* for sample S-1), from which η_0 can be estimated. However, the extrapolation based on eq. (7) should be made carefully because, as mentioned above, the range of shear stress where the linear relationship holds differs with the sample characteristics (chain branching, molecular weight, and molecular weight distribution).

Method 2 did not give good results (Fig. 5). Care should be taken in application of this method, although it is frequently used for estimating η_0 for practical purposes.

Plots of method 3 give straight-line relationships over the relatively broad range of shear rate. The straight lines drawn are those calculated by the least-squares method from data points in the shear stress range of $10^5 < \tau < 6 \times 10^5$ dynes/cm.^{2}. The upper limit is added because τ_d, the critical shear stress for flow irregularity, was about 6×10^5 dynes/cm.^{2} for sample D-1. The applicability of this method (method 3) is quite

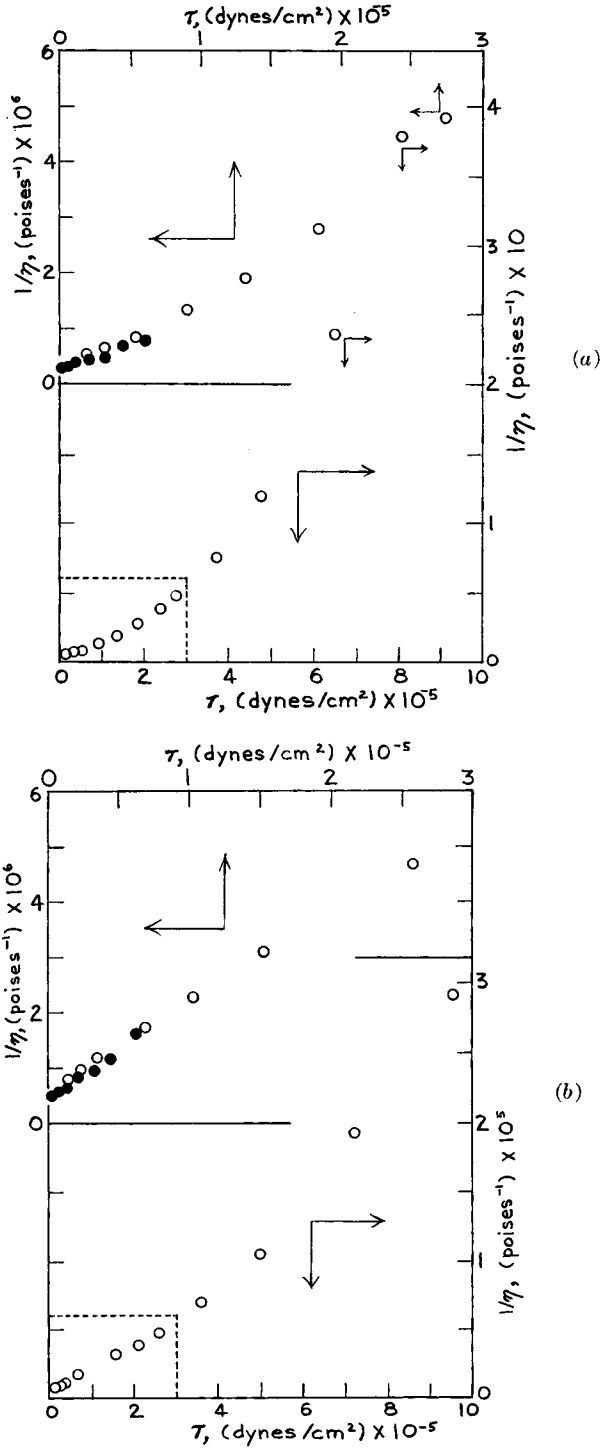

Fig. 4. (*a*) Plot of $1/\eta$ versus τ for sample D-1 (the portion enclosed by dotted lines is enlarged in the upper graph): (O) capillary data; (●) cone–plate data. (*b*) Plot of $1/\eta$ versus τ for sample S-1 (the portion enclosed by dotted lines is enlarged in the upper graph): (O) capillary data; (●) cone-plate data.

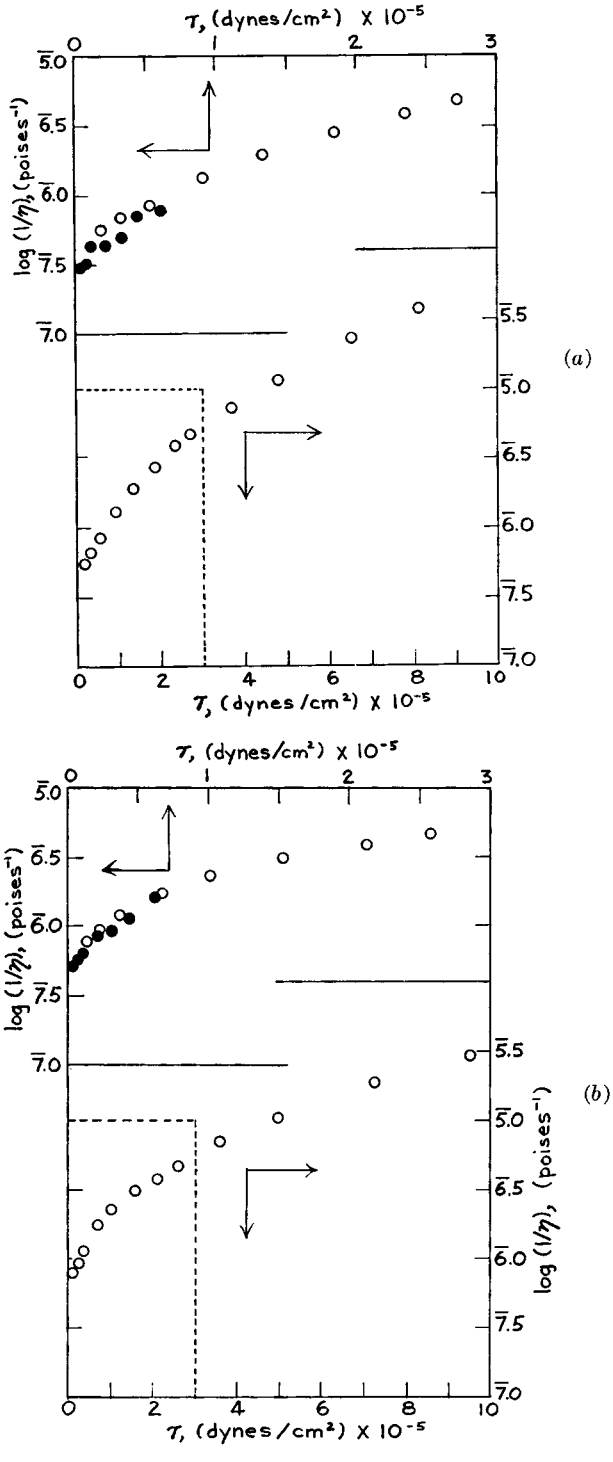

Fig. 5. (*a*) Plot of log $1/\eta$ versus τ for sample D-1 (the portion enclosed by dotted lines is enlarged in the upper graph): (O) capillary data; (●) cone–plate data. (*b*) Plot of log $1/\eta$ versus τ for sample S-1 (the portion enclosed by dotted lines is enlarged in the upper graph): (O) capillary data; (●) cone–plate data.

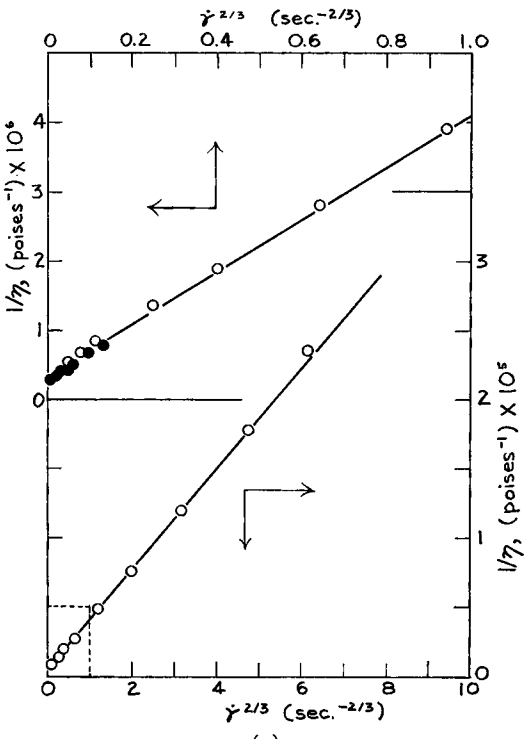

(a)

Figure 6. See caption p. 951.

satisfactory for sample D-1 but is not necessarily so for sample S-1, as shown in the enlarged-scale plots. From the intercept of the line the zero shear viscosity η_0 is calculated. The observed and calculated values of η_0 are given in columns 4 and 5 in Table V. Both values for the D series samples agree approximately, but the calculated values for the other samples are about half of the observed values. Nevertheless, this method seems to be valuable, because it gives the value η_0 within a factor of about 2 by extrapolating viscosity data at shear stress between 10^5 and 6×10^5 dynes/cm.^{2}.

The exponent of $\dot{\gamma}$ in eq. (9) is, in the original form,[21] set equal to p/q, where p is an even integer and q is an odd integer. Cross found that the value $^2/_3$, the simplest case, gave good results for many systems. As the effect of shear rate on flow properties depends largely on the molecular weight distribution,[23-25] it seems to be somewhat oversimplified that p/q takes only a single value $^2/_3$ in all cases, irrespective of molecular weight distributions (or, in general, sample characteristics). If the value p/q varies, the practical utility of the equation is largely lessened.

Elastic Properties

The total end correction e consists of a purely geometric part m, the Couette correction, and of an elastic deformation in shear, S_R, the re-

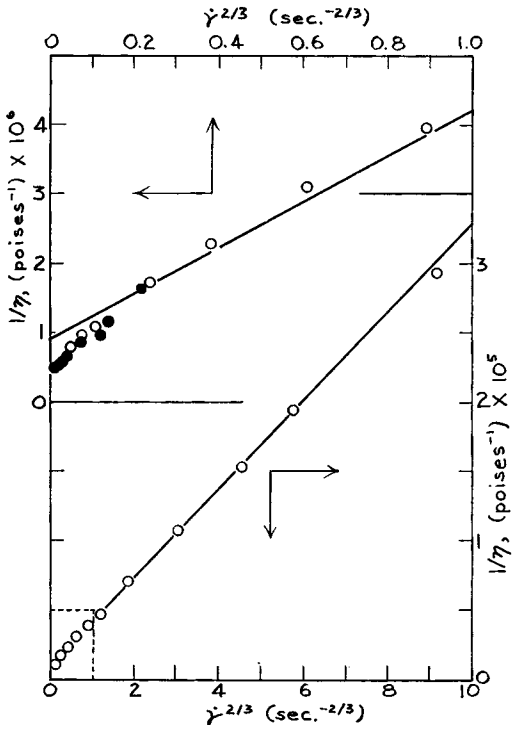

(*b*)

Fig. 6. (*a*) Plot of $1/\eta$ versus $\dot{\gamma}^{2/3}$ for sample D-1 (the portion enlosed by dotted lines is enlarged in the upper graph); the straight line is that calculated by the least-squares method from data points in the range of $10^5 < \tau < 6 \times 10^5$ dynes/cm.^{2}. (*b*) Plot of $1/\eta$ versus $\dot{\gamma}^{2/3}$ for sample S-1 (the portion enlosed by dotted lines is enlarged in the upper graph); the straight line is that calculated by the least-squares method from data points in the range of $10^5 < \tau < 6 \times 10^5$ dynes/cm.^{2}.

coverable shear strain:

$$e = m + {}^1/_2 S_R \tag{10}$$

As shown in Figure 3, the value e is about 1 at sufficiently low shear rate; it may be that the value of m is the same as that of the Newtonian liquid. We used the value[26] 0.77 for m and calculated S_R.

On the other hand, S_R is given by the relation

$$S_R = J_e \tau \tag{11}$$

where J_e is the steady-state compliance obtained with the cone–plate viscometer.

In Figure 7 values of S_R for samples D-1, D-2, S-1, and S-3 are plotted against τ. The values determined with both apparatuses fall on practically the same curves. Hook's law in shear holds at the shear stress below about 10^4 dynes/cm.^{2}.

The shear modulus μ is given as

$$\mu = \tau/S_R \tag{12}$$

The value of μ was nearly constant at a shear stress of about 10^4 dynes/cm.^{2} and then increased slightly with shear stress, until τ_d. Above the critical shear stress τ_d the value μ for low-density samples increased approximately proportionally to shear stress. Values of μ at two levels of shear stress are given in columns 7 and 8 of Table V. The value μ is much higher for the high-density polyethylene than for the low-density, and μ is higher for

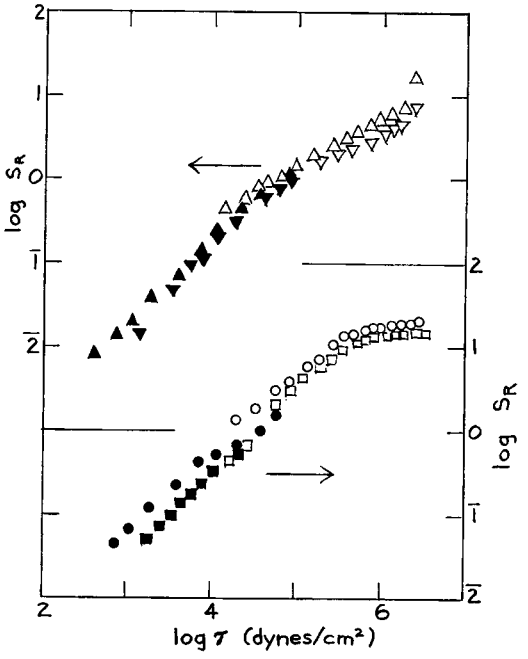

Fig. 7. Recoverable shear strain s_r versus shear stress for samples: (O) D-1; (□) D-2; (△) S-1; (▽) S-3. Capillary data are shown with open symbols and cone–plate data with closed.

lower molecular weight samples than for higher molecular weight species. The effect of temperature on μ was not clear in the data of sample D-2.

The internal shear modulus of rigidity G_i, defined by eq. (7), is given in column 9 of Table V. The value G_i is approximately proportional to μ if a comparison is made among the same type of samples (D-series or S-series), but G_i for the S series sample (high-density polyethylene) is, contrary to the case of μ, less than that of the D series sample (low-density polyethylene). Care should be taken when G_i is treated as the measure of elasticity.

References

1. J. R. Van Wazer, J. W. Lyons, K. Y. Kim, and R. E. Colwell, *Viscosity and Flow Measurement*, Interscience, New York, 1963.
2. W. Philippoff and F. H. Gaskins, *Trans. Soc. Rheol.*, **2**, 263 (1958).
3. F. D. Dexter, *J. Appl. Phys.*, **25**, 1124 (1954).
4. W. Philippoff and F. H. Gaskins, *J. Polymer Sci.*, **21**, 205 (1956).
5. L. H. Tung, *J. Polymer Sci.*, **46**, 409 (1960).
6. E. B. Bagley, *J. Appl. Phys.*, **28**, 624 (1957); *idem., Trans. Soc. Rheol.*, **5**, 355 (1961).
7. J. P. Tordella, *Trans. Soc. Rheol.*, **1**, 203 (1957).
8. L. Marker, R. Early, and S. L. Aggarwal, *J. Polymer Sci.*, **38**, 381 (1959).
9. H. P. Schreiber, E. B. Bagley, and D. C. West, *Polymer*, **4**, 355 (1963).
10. H. P. Schreiber, *J. Appl. Polymer Sci.*, **4**, 38 (1964).
11. T. Kataoka, *Bull. Textile Res. Inst. (Japan)*, **64**, 71 (1963).
12. T. Kataoka, *J. Appl. Polymer Sci.*, in press.
13. T. Arai, *A Guide to the Testing of Rheological Properties with the Koka Flow Tester*, Maruzen, Tokyo, 1958.
14. L. H. Tung and S. Buckser, *J. Phys. Chem.*, **62**, 1530 (1958).
15. R. E. Powell and H. Eyring, *Nature*, **154**, 427 (1944).
16. R. S. Spencer and R. E. Dillon, *J. Colloid Sci.*, **3**, 163 (1948).
17. Y. H. Pao, *J. Appl. Phys.*, **28**, 591 (1957).
18. F. Bueche and S. W. Harding, *J. Polymer Sci.*, **32**, 177 (1958).
19. W. W. Graessley, *J. Chem. Phys.*, **43**, 2696 (1965).
20. T. Gillespie, *Trans. Soc. Rheol.*, **9**:**2**, 35 (1965).
21. M. M. Cross, *J. Colloid Sci.*, **20**, 417 (1965); *idem., European Polymer J.*, **2**, 299 (1966).
22. J. D. Ferry, *J. Am. Chem. Soc.*, **64**, 1330 (1942).
23. H. P. Schreiber, *J. Appl. Polymer Sci.*, **9**, 2101 (1965).
24. R. L. Ballman and R. H. M. Simon, *J. Polymer Sci. A*, **2**, 3557 (1964).
25. S. Middleman, *J. Appl. Polymer Sci.*, **11**, 417 (1967).
26. S. Iwanami, *Trans. Japan. Soc. Mech. Engrs.*, **18**, 52, 59 (1952).

Received August 28, 1967